

## Site-selective laser-spectroscopy studies of the intrinsic 1.9-eV luminescence center in glassy SiO<sub>2</sub>

Linars Skuja

*Institute of Solid State Physics, University of Latvia, Riga LV1063, Latvia*

Toshio Suzuki and Katsumi Tanimura

*Department of Physics, Nagoya University, Furo-cho, Chikusa, Nagoya 464-01, Japan*

(Received 8 May 1995)

The intrinsic 1.9-eV photoluminescence band (the *R* band) in neutron-irradiated synthetic silica glass has been studied using site-selective photoluminescence excitation in the 2.0 eV absorption band and transient spectral hole-burning techniques. The measurements of the low-energy wing of the zero-phonon line intensity distribution function confirm the predicted nearly Gaussian shape with a peak at 1.93 eV and a half-width of 86 meV. The homogeneous shape of the emission contour ("single-site spectrum") has been evaluated by a selective saturation method, revealing, a phonon sideband with a peak at 60 cm<sup>-1</sup> and a width of approximately 500 cm<sup>-1</sup>. The total Huang-Rhys factor is estimated as 1.50±0.5 and the partial Huang-Rhys factor for the interaction with the 890 cm<sup>-1</sup> local vibration is 0.08±0.04. The analysis of spectral parameters indicates that the *R* band cannot be due to peroxide or ozonide molecular ions and upholds the attribution of the center to the nonbridging oxygen hole center.

### I. INTRODUCTION

The photoluminescence (PL) band with the peak around 1.9 eV, which is associated with excitation and absorption bands at 2.0 and 4.8 eV, is universally present in neutron,<sup>1</sup>  $\gamma$ ,<sup>2</sup> electron,<sup>3</sup> x-ray,<sup>1,4</sup> or ultraviolet (UV) irradiated<sup>5,6</sup> glassy SiO<sub>2</sub> (*g*-SiO<sub>2</sub>). This band is also induced by drawing SiO<sub>2</sub> into fibers<sup>7</sup> or ion implantation.<sup>8</sup> Defect centers on the surface of mechanically fractured silica give rise to a similar PL band.<sup>9</sup> Although its spectrum was first reported a long ago,<sup>3</sup> the basic structural model of the associated defect center and assignment of its electronic transitions are still a matter of discussions. It is generally agreed only that the center is due to an oxygen-excess-related intrinsic defect in *g*-SiO<sub>2</sub>. Two different basic models and their variations are presently discussed: the nonbridging oxygen hole center<sup>1,4,10</sup> (NBOHC, dangling oxygen bond with a hole in its non-bonding  $\pi$  orbital) and an interstitial oxygen atom produced in the photolysis of interstitial ozone molecules.<sup>6</sup> The available experimental data and proposed models have been reviewed recently in Refs. 11 and 12.

The peak energy of the 1.9-eV PL band shifts between 1.8 and 2 eV,<sup>12</sup> depending on the excitation wavelength within the 2-eV absorption band. Other bands of possibly related origin have been observed in the 2.0–2.05 eV region.<sup>12,13</sup> On the other hand, defect centers of an entirely different nature also give rise to emission bands within this spectral range.<sup>14</sup> To avoid confusion in notation and in view of the controversy over the structural model of the "1.9-eV" PL center, we shall use here instead neutral names "*R* center" and "*R* band," as suggested in Ref. 12. Employing only those data which are presently generally accepted, the *R* band can be defined most exactly as the (red) PL band due to intrinsic defects in *g*-SiO<sub>2</sub> with a peak at 1.9±0.1 eV, excitation band at 2±0.1 eV, and decay time constant distributed between 10 and 30  $\mu$ s at room temperature. The character of the 4.8-eV excitation band of the *R* center, which appears also as a strong optical absorption band in irradiated oxygen-excess *g*

-SiO<sub>2</sub>, has remained particularly controversial. It was originally attributed to the  $\sigma \rightarrow n$  type transition of the NBOHC.<sup>15</sup> However, a number of other researchers have come to a different conclusion, that 4.8-eV absorption band is not an inherent feature of the *R* center and is caused rather by some other defect<sup>5,6,13,16,17</sup> with the *R*-band excitation occurring subsequently via energy transfer.

Additional data, contributing to a deeper understanding of the *R* center, were recently obtained using site-selective laser excitation in the 2.0-eV optical absorption band at liquid helium temperatures<sup>10</sup> (a detailed account of the work can be found in Ref. 12). Highly polarized resonance zero-phonon lines (ZPL's) and satellite lines 50 and 890 cm<sup>-1</sup> apart were discovered. The ZPL was attributed to a charge-transfer transition of the hole from the semidegenerate NBOHC lone-pair 2*p* orbital to the lone-pair orbital of one of the three adjacent oxygen atoms sharing the same SiO<sub>2</sub> tetrahedron.<sup>10,12</sup> The 890-cm<sup>-1</sup> line was suggested to be due to the coupling to the silicon–nonbridging-oxygen symmetric stretching mode in the electronic ground state. The 50-cm<sup>-1</sup> mode was not assigned. The dependence of the intensities of ZPL's on excitation photon energies was measured between 1.91 and 2.01 eV and yielded a nearly Gaussian distribution with a peak at 1.93 eV and halfwidth 82 meV. The low-energy wing of the distribution, however, has not been investigated. The site-selective PL spectra of the *R* center<sup>10,12</sup> have revealed many spectral details which are smeared out by the inhomogeneous broadening in the conventional PL spectrum. However, the true spectral shape of the homogeneous ("single-site") PL spectrum, important for the theoretical analysis of the *R* center, is still not known.

The site-selective PL emission spectra generally consist of two components: the homogeneous part due to excitation of sites with ZPL's in resonance with the excitation photon energy and the inhomogeneous part due to the nonselective excitation of the centers at other sites, for which the excitation-photon energy falls within the absorption spectrum phonon sideband. If one assumes that the spectra origi-

nating from PL centers at different sites experience just site-dependent energy shifts, but have the same, site-independent, set of other parameters, then the dependence of the PL intensity  $I$  on excitation ( $E_{\text{exc}}$ ) and emission ( $E_{\text{em}}$ ) energies is given by

$$I(E_{\text{em}}, E_{\text{exc}}) = \int_0^{\infty} W(\varepsilon) K(E_{\text{exc}} - \varepsilon) L(E_{\text{em}} - \varepsilon) d\varepsilon, \quad (1)$$

where  $K(E)$  and  $L(E)$  are the site-independent (homogeneous) contours of the excitation and emission spectra, defined in coordinates where  $E=0$  corresponds to the ZPL.  $W(E)$  is the probability that a PL center at an arbitrary site has ZPL energy  $E$ .

From the viewpoint of the basic site-selective fluorescence theory (e.g., Ref. 18), the inhomogeneously broadened component of the PL spectrum is commonly expected to be suppressed more effectively when excitation takes place as far as possible in the low-energy wing of the ZPL distribution  $W(E)$ . However, this region was not investigated in previous studies,<sup>12</sup> since the excitation energies below 1.905 eV were not available.

The site selectivity can be further improved by site-selective fluorescence saturation techniques (e.g., Refs. 19 and 20). It is based on the idea that the homogeneous component of the site-selective emission spectrum, which is excited via ZPL's, on increasing of laser excitation density saturates more easily than the inhomogeneous component, excited via phonon sidebands (PSB's). Alternatively, this may be viewed as a transient resonance spectral hole burning in the excitation spectrum of the centers. The saturating component  $I_{\text{sat}}$  is defined as a difference between two normalized PL spectra, measured at two different laser excitation densities  $D_1$  and  $D_2$  ( $D_1 < D_2$ ):

$$I_{\text{sat}} = I_1/D_1 - I_2/D_2. \quad (2)$$

For the case of a laser pulse much shorter than the lifetime of the excited state,

$$I_{\text{sat}} \propto N \left[ \frac{1 - \exp(-\sigma D_1)}{D_1} - \frac{1 - \exp(-\sigma D_2)}{D_2} \right], \quad (3)$$

where  $N$  is the concentration of PL centers with absorption cross section  $\sigma$  at laser wavelength and  $D$  is expressed in [photon/cm<sup>2</sup>] units. Because of the inhomogeneous broadening, the resulting luminescence consists of two components with different saturation properties. The "homogeneous" part of the luminescence spectrum corresponds to the fraction of sites having ZPL's coincident with the laser photon energy, with the absorption cross section  $\sigma_Z$  and concentration  $N_Z$ . The "inhomogeneous" part of the emission spectrum is due to a much larger number ( $N_P$ ) of sites which have PSB's in the absorption spectrum at the laser energy with a mean absorption cross section  $\sigma_P$  ( $\sigma_P \ll \sigma_Z$ ). From Eq. (3) it follows that in the weak excitation limit ( $\sigma D \ll 1$ ) the ratio  $P$  between the intensities of homogeneous and inhomogeneous saturated components is

$$P = \frac{I_{\text{sat}}^{\text{hom}}}{I_{\text{sat}}^{\text{inh}}} \approx \frac{N_Z \sigma_Z^2}{N_P \sigma_P^2} = \frac{N_Z \sigma_Z}{N_P \sigma_P} \left( \frac{\sigma_Z}{\sigma_P} \right). \quad (4)$$

The ratio  $N_Z \sigma_Z / N_P \sigma_P$  can be roughly estimated from the conventional (nonsaturated) site-selective spectra as the ratio between the integral intensities of ZPL's and the broad composite sideband. For the case of 1.905 eV excitation of the  $R$  center in silica, this ratio is approximately 0.06.<sup>12</sup> On the other hand, for defects with medium to weak electron-phonon coupling (Huang-Rhys factors  $S < 3$ ) the ratio between the absorption cross sections of ZPL's and PSB's,  $\sigma_Z / \sigma_P$ , is much higher,  $10^4 - 10^5$ .<sup>19</sup> Thus the ratio  $P$  in Eq. (4) exceeds  $10^2 - 10^3$  and the saturated component is practically completely due to the homogeneous (single-site) PL emission spectrum.

The objectives of the present paper are (1) to explore the site-selective PL of the  $R$  center using the theoretically most interesting region of the low excitation energies and to obtain the low-energy wing of the zero-phonon line distribution function and (2) to evaluate the homogeneous lineshape of the  $R$  band, using transient spectral hole burning through fluorescence line saturation. Based on the experimental results, the structural model of the  $R$  center is discussed, and the possible relation between the  $R$  center and PL centers which give rise to 2.05-eV band<sup>12,13</sup> in irradiated glassy SiO<sub>2</sub> is explored.

## II. EXPERIMENT

The glassy SiO<sub>2</sub> sample used in this study was synthetic high-purity "wet" commercial silica Corning 7940 of dimensions  $8 \times 8 \times 4$  mm<sup>3</sup>, irradiated by  $10^{20}$  neutron/cm<sup>2</sup>. The sample was placed in the liquid-He cryostat of the cold finger type, with the temperature being between 6 and 8 K during measurements. Luminescence was excited by 20-ns long pulses from an excimer-laser-pumped dye laser (Lambda Physik EMG201MSC and FL3002) with DCM (range 1.79–1.94 eV) and Coumarin 153 (range 2.187–2.50 eV) dyes. Neutral density glass filters were used for variable-beam attenuation in the selective saturation experiments, and the beam intensity was monitored by a Si photodiode and a boxcar averager. The emission light was collected at a right angle to the excitation beam, dispersed by a triple monochromator spectrograph (SPEX Triplemate) (600 line/mm gratings both in filter and spectrograph stages) and detected by a gated optical multichannel analyzer (1024-channel image-intensified diode array Princeton IRY 1024). To reject the scattered laser excitation light, a gate of 30  $\mu$ s width delayed 3  $\mu$ s after the laser pulse was applied to the detector. Up to 3000 laser pulses were averaged at repetition frequency 1–2 Hz to obtain the required single-to-noise ratio. It was verified that neither sample warming nor permanent spectral hole burning took place during the measurements. Since the width of the spectral region of interest was larger than the maximal bandwidth of the spectrograph filtering stage (ca. 40 nm), two partially overlapping sections of spectra centered at different wavelengths were routinely taken. They were assembled together by multiplying the lower-energy spectrum by an appropriate factor to match their integrals in the mutual overlap region.

To control the nonlinear saturation effects and to select the optimal laser power density for selective saturation experiments, sets of PL spectra were recorded with different power densities at each excitation wavelength. The depen-

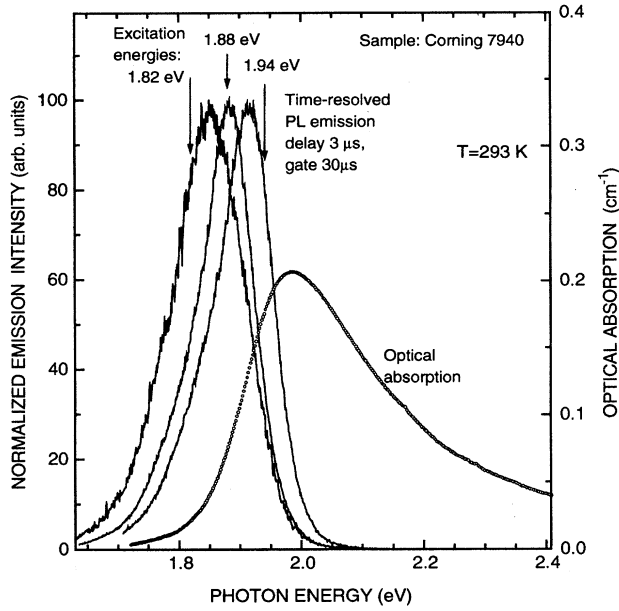


FIG. 1. Optical absorption of neutron-irradiated Corning 7940 synthetic  $\text{SiO}_2$  glass (the right scale) and time-resolved luminescence spectra measured under pulsed dye laser excitation at 1.82, 1.88, and 1.94 eV. Emission spectra are independently normalized to the same height.  $T=293$  K.

dences of the PL intensity  $I$  on laser power density  $D$  were fitted by the simplest model function

$$I \propto 1 - \exp(-\sigma D), \quad (5)$$

where  $\sigma$  is the absorption effective cross section and  $D$  is expressed in [ $\text{photon}/\text{cm}^2$ ] units and delivered in a time much shorter than the PL decay constant. The focusing conditions of the excitation light were initially adjusted at each excitation wavelength to obtain maximum values (i.e., without attenuating filters) of  $\sigma D$  in the region of 1.5–2. Spectra with lower excitation power densities were subsequently obtained using calibrated neutral density glass absorption filters.

It was found during the selective saturation experiments that the linearity of the signals from the image-intensified detector was insufficient to obtain reliably the saturated component in the usual<sup>20</sup> straightforward way, as the difference between the low-intensity and high-intensity emission spectra, normalized to their respective excitation intensities [Eq. (2)]. To overcome this obstacle, the spectrum of the saturated component  $L_{\text{sat}}(\lambda)$ , measured with laser excitation wavelength  $\lambda_{\text{las}}$ , was calculated as

$$L_{\text{sat}}(\lambda) \propto L_1(\lambda) - L_2(\lambda) \frac{T(\lambda_{\text{las}})}{T(\lambda)} = L_1(\lambda) - L_{2K}(\lambda), \quad (6)$$

where  $L_1(\lambda)$  and  $L_2(\lambda)$  are two subsequent luminescence spectra taken first with the neutral density attenuating filter of transmissivity  $T(\lambda)$  placed in the exciting laser beam ( $L_1$ ) and then with the same filter transferred to the emission beam ( $L_2$ ). This technique ensured that nearly the same light intensities reached the detector in both measurements and

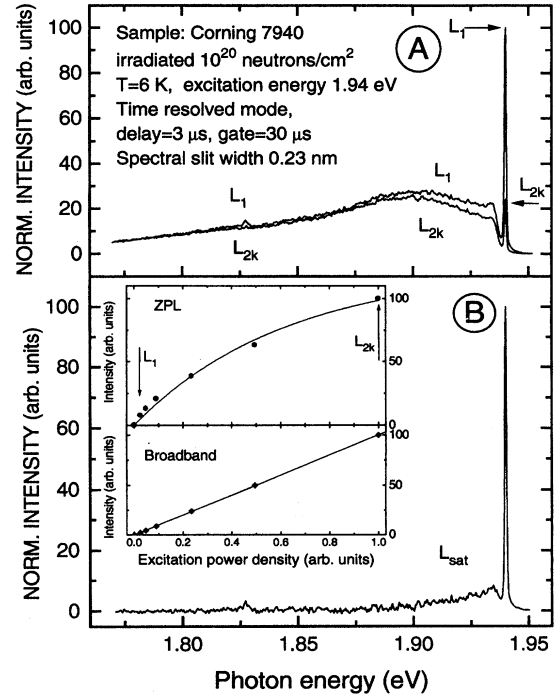


FIG. 2. (a) Low-temperature time-resolved luminescence spectra measured at low (spectrum  $L_1$ ) and high (spectrum  $L_{2k}$ ) excitation power density and normalized to the respective intensities of the excitation light according to Eq. (6). Horizontal arrows indicate the amplitudes of the zero-phonon lines. (b) Saturated component of the emission spectrum (single-site spectrum)  $L_{\text{sat}} = L_1 - L_{2k}$ . The inset shows the dependence of the emission intensity on the excitation density measured on the zero-phonon line (upper part) and on the broadband low-energy tail of the emission spectrum (lower part). The vertical arrows in the inset indicate the excitation densities used to measure the emission spectra  $L_1$  and  $L_{2k}$  of part (a). Excitation photon energy 1.94 eV.

thus canceled most of the nonlinearity. Attenuation filters were calibrated using a Shimadzu UV3100 spectrophotometer.

During the measurements of the dependence of ZPL intensity on wavelength, the laser power was kept sufficiently low to avoid saturation. To correct the measured dependence both for the spectral variations of laser power and the spectral sensitivity of the detection system, the intensity of Rayleigh scattering  $R(\lambda)$  was recorded at each laser wavelength  $\lambda$  using a  $\text{CCl}_4$  solution in a quartz cell placed at the sample site. The subsequently measured ZPL intensities were normalized by  $\lambda^4 R(\lambda)$ .

### III. RESULTS

Room-temperature time-resolved PL spectra of neutron-irradiated  $g$ - $\text{SiO}_2$ , measured with excitation at three different energies (1.82, 1.88, and 1.94 eV) in the low-energy part of the resonance absorption region are shown in Fig. 1. The peak positions of the PL emission spectra are dependent on the excitation energy used and PL spectra are much narrower than the optical absorption spectrum. The absence of a sharp line at the excitation energy confirms that the interference

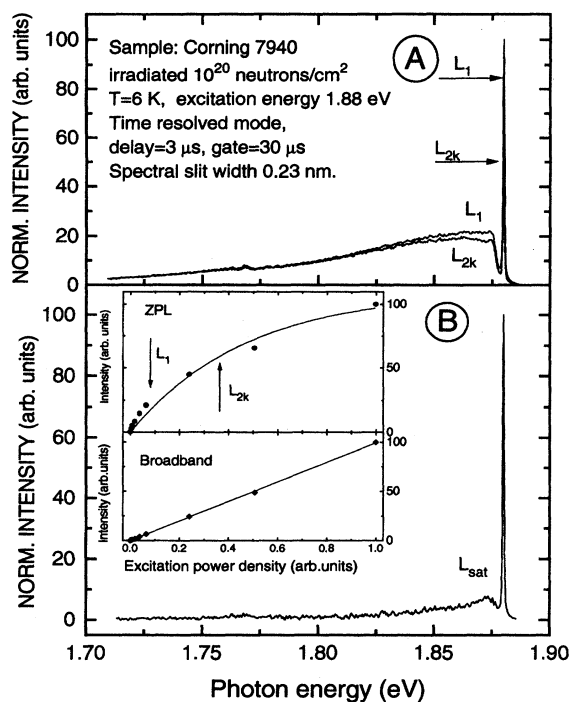


FIG. 3. The same as Fig. 2, excitation photon energy 1.88 eV.

from the elastically scattered laser light is completely suppressed by the gating techniques.

When the luminescence spectra are recorded at 6 K, the PL emission consists of a sharp resonance zero-phonon line and a broad sideband [parts (a) of Figs. 2–4], as previously<sup>10,12</sup> reported. Figure 5 shows the measured dependence of the integrated intensities of ZPL's on the excitation energy in the 1.80–1.94 eV region. During these measurements, the excitation density was kept sufficiently low to avoid line saturation. The previously measured<sup>12</sup> high-energy part of the ZPL distribution is also shown (Fig. 5, circles). Both data sets were normalized to fit in their mutual overlap region (1.90–1.94 eV). A least-squares Gaussian fit to the resulting joint distribution gave a distribution peak at 1.93 eV and halfwidth 0.086 eV.

Contrary to the initial expectations, the measurements performed with the excitation in the extended low-energy wing of the ZPL distribution ( $h\nu=1.82$  eV) did not yield dramatically better resolved line structures as compared to spectra obtained at higher excitation energies (compare Figs. 2–4). The previously reported<sup>10,12</sup>  $890\text{-cm}^{-1}$  vibrational structure is present in all spectra; the sharp line  $\approx 50\text{ cm}^{-1}$  below the ZPL (Ref. 12) is even somewhat less evident in the 1.82-eV excited spectrum as compared to the 1.94-eV excited spectrum (Figs. 4 and 2).

The dependences of the ZPL's and the broad sideband intensities on the incident laser power measured at excitation energies 1.82, 1.88, and 1.94 eV are shown in the insets of Figs. 2(b), 3(b), and 4(b). The sideband intensities were monitored as integrals over regions of spectra between 0.14 and 0.12 eV below the ZPL energy. The intensities of the ZPL's exhibit a typical saturation behavior, roughly consistent with Eq. (5), while at the same power levels the inte-

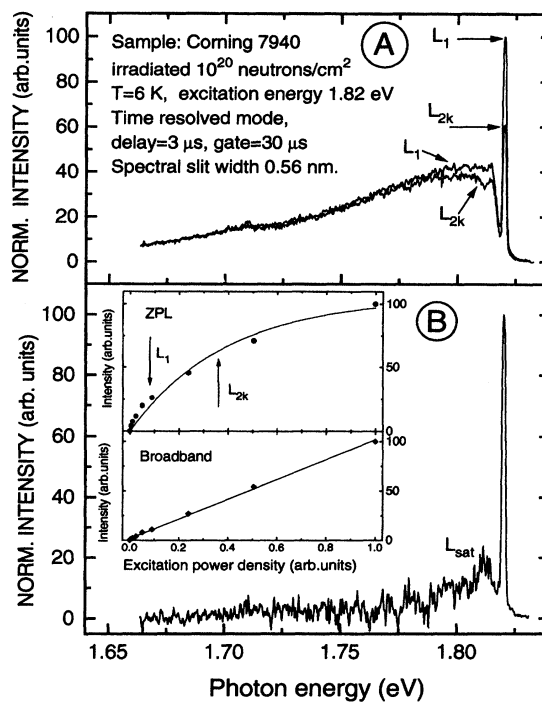


FIG. 4. Same as Fig. 2, excitation photon energy 1.82 eV.

grated intensities of the broad sideband retained practically linear laser power dependence.

Parts (a) of Figs. 2–4 show the comparison of site-selective PL spectra measured at two different excitation densities for photon energies 1.82, 1.88, and 1.94 eV and normalized to the respective excitation densities. Their difference (the saturated component spectrum) calculated according to Eq. (6) is shown in parts (b) of the figures. The excitation densities used to obtain the high-intensity and low-intensity spectra are indicated by arrows on the saturation curves in the insets. Initially, while taking data for Figs.

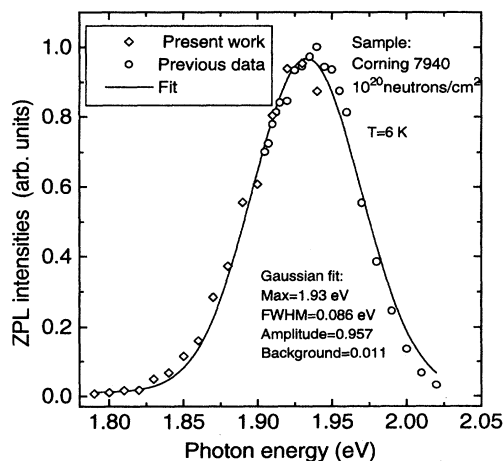


FIG. 5. Dependence of resonance zero-phonon line intensities on excitation photon energy. Experimental data points for the high-energy part are taken from Ref. 12.

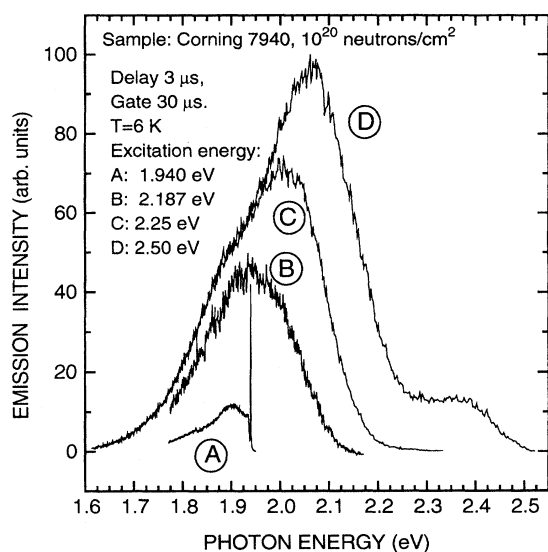


FIG. 6. Time-resolved site-selective luminescence spectra of neutron-irradiated synthetic silica, measured at excitation energies 1.940, 2.187, 2.25, and 2.50 eV.

3 and 4, relatively shallow saturation was used, in order to ensure that only the homogeneous part of the spectrum is saturated [Eq. (4)]. However, it was found during the measurements that the broadband did not saturate and the shape of the saturated spectrum did not change also when higher intensities were used. The data for Fig. 2 were measured with higher excitation density (deeper saturation) and yielded a better signal-to-noise ratio for the saturated component spectrum. Time-resolved PL spectra measured at excitation in the 2.187–2.5 eV region are shown in Fig. 6. Apart from the *R* band, PL bands at 2.05–2.08 and 2.35–2.4 eV are present at this excitation, in agreement with Ref. 12. Vibrational structures or resonances ZPL's connected to these bands were not visible above the noise level.

#### IV. DISCUSSION

##### A. Distribution of zero-phonon lines

Under the model simplifications described in the Introduction and leading to Eq. (1), the dependence of the ZPL intensity on resonance excitation photon energy (“ZPL excitation spectrum”) is proportional<sup>21</sup> to the site energy distribution function  $W(E)$  in Eq. (1) (see, however, Ref. 22). The measured low-energy wing of the ZPL intensity distribution agrees well with the previously obtained<sup>12</sup> data for the central and high-energy parts of the distribution (Fig. 5). The finding that the distribution is approximated by a single Gaussian indicates that the luminescence is due to a single type of defect, undergoing continuous inhomogeneous broadening, and most likely is not due to a superposition of several discrete modifications of the *R* center, present in comparable concentrations. A likely candidate for such a modification, the 2.05-eV PL band, which by spectral position, halfwidth, and lifetime [ $\approx 10 \mu\text{s}$  (Ref. 12)] looks very similar to the *R* band, seems to have no ZPL's (at least intense ones) (Fig. 6). However, the excitation energy region

between 2.04 and 2.10 eV, which was not available in the present work, should be scrutinized carefully before a firm conclusion can be drawn that the *R* and 2.05-eV bands have entirely different origins. The high-energy PL band at 2.35 eV definitely exhibits no resonance ZPL's. However, both 2.15- and 2.35-eV PL centers can contribute to the “2.0-eV” optical absorption band (Fig. 1), which should be taken into account when electron paramagnetic resonance (EPR) optical absorption correlations are searched for.

The halfwidth of the distribution  $W(E)$ , 86 meV ( $\approx 690 \text{ cm}^{-1}$ ), is in agreement with the previous estimate,  $82 \pm 7 \text{ meV}$ ,<sup>12</sup> based on the fit to the high-energy wing of the distribution. It is significantly larger than in most glass-activator systems, investigated by the fluorescence line-narrowing techniques: for example,  $\approx 25 \text{ cm}^{-1}$  in  $\text{Yb}^{3+}$ -doped silica glasses,  $\approx 50 \text{ cm}^{-1}$  in  $\text{Nd}^{3+}$ -doped phosphate glasses,<sup>18</sup>  $\approx 200 \text{ cm}^{-1}$  in  $\text{Cr}^{3+}$ -doped silicate glasses,<sup>23</sup> and typically of order  $200 \text{ cm}^{-1}$  in organic-dye-doped polymers<sup>20</sup> and frozen solutions.<sup>21</sup>

Estimates of the halfwidth of  $W(E)$  for ground-to-excited-state splittings in several intrinsic defects in *g*- $\text{SiO}_2$  have been performed also by computer simulations of the electron paramagnetic resonance spectra.<sup>24</sup> For peroxide radical defects the distribution halfwidth is  $460 \text{ cm}^{-1}$ , while for NBOHC values as high as  $4000 \text{ cm}^{-1}$  were needed to fit the calculated to the experimental NBOHC EPR spectrum. However, the latter value does not automatically conflict with the value obtained from the luminescence data of the present work, since the excited states which contribute to the *g* shifts and the excited states active in the optical transitions are different. The biggest *g* shift in the NBOHC is caused by the low-lying excited state due to the transition of the unpaired electron between both semidegenerate  $2p$  orbitals of the nonbridging oxygen atom,<sup>24</sup> while the optical transition is assigned<sup>10,12</sup> to the charge-transfer transition of the hole to the lone pair  $2p$  orbital of the neighboring oxygen atom.

##### B. Homogeneous shape of the *R* band

Figure 7 and parts (b) of Figs. 2–4 show the comparison between the normalized spectra of saturated components, measured at three different excitation energies. Within the measurements accuracy the shape of the saturated component spectrum is independent of the excitation energy. This confirms that the approximations described in the Introduction are justified and the saturated component spectra within the accuracy limits describe the single-site (homogeneous) shape of the *R* band.

The integral intensity of the ZPL,  $I_{\text{ZPL}}$ , relative to the total integral intensity of the emission band  $I_0$ , is given by

$$I_{\text{ZPL}} = I_0 \exp(-S), \quad (7)$$

where  $S$  is the Huang-Rhys factor.<sup>25</sup>  $S$  values calculated according to Eq. (7) from spectra in Figs. 2(b), 3(b), and 4(b) are 0.99, 1.40, and 1.35, respectively. Since the phonon wing is very weak, the main source of errors in calculating  $S$  is the sensitivity to inaccuracies in background subtraction. Lowering of the background line by 1% in Fig. 2(b) increased the calculated  $S$  value from 0.99 to 1.30. We estimate the mean value of  $S$  as  $1.4 \pm 0.5$ . Although relatively high excitation densities were used and conditions for Eq. (4) were not ex-

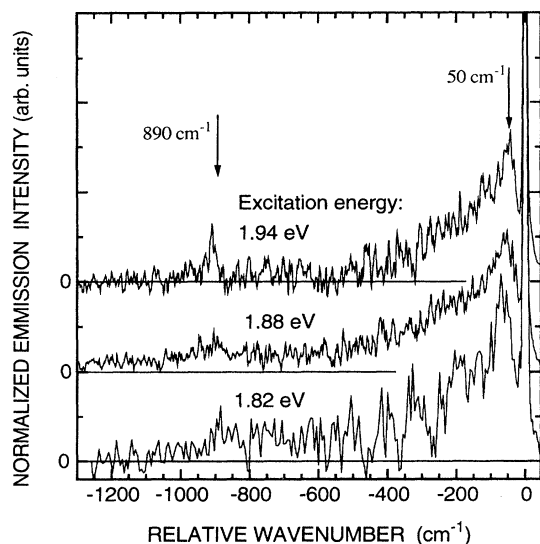


FIG. 7. Comparison of the band shapes of the saturated components (phonon sidebands of single-site spectra), measured at excitation energies 1.82, 1.88, and 1.94 eV. All spectra have been normalized to the same height of the respective zero-phonon lines (here off scale). The 1.82-eV spectrum has been corrected for the different spectrograph slit width.

actually valid, there were no signs of saturation in the broad sidebands (insets in Figs. 2–4). Therefore the admixture of the inhomogeneous component to the saturated spectra should be negligible. In any case the calculated values of  $S$  represent the *upper limit* to the Huang-Rhys factor of the  $R$  center.

In a simplified configuration coordinate model, assuming an effective linear coupling of the electronic transition to a single-vibration mode (e.g., Ref. 25), the Stokes shift is  $2S$  times the vibration energy quantum  $h\omega$ . With a Stokes shift of the  $R$  center of  $\sim 0.09$  eV ( $\sim 725$   $\text{cm}^{-1}$ ), this corresponds to a mean effective  $h\omega$  of 250–300  $\text{cm}^{-1}$ , which agrees reasonably with the surface phonon spectrum of the oxygen-terminated surface of  $\text{SiO}_2$ .<sup>26</sup>

As already pointed out in a preceding paper,<sup>12</sup> the  $R$  center represents the first instance of ZPL's and vibrational structures, observed for intrinsic defects in undoped oxide glasses. To our knowledge, no such structures have been reported so far also in the closest crystalline analog of glassy  $\text{SiO}_2$ ,  $\alpha$  quartz. ZPL's have been observed in some other oxide crystals with mixed ionic-covalent bonding (e.g., neutron-irradiated  $\text{Al}_2\text{O}_3$  crystals<sup>27,28</sup>) or ionic bonding [ $F^+$  center in  $\text{CaO}$  (Ref. 25)]. However, the reported values of Huang-Rhys factors for the respective centers are much larger, 5.0–5.9 (Ref. 27) and 4.0–6.0,<sup>25</sup> in compliance with the usual notion that oxide materials are generally characterized by a relatively strong electron-phonon coupling. The  $S$  values obtained for the  $R$  center in the present work can thus be regarded as anomalously small.

### C. Nature of the phonon sideband

The previously reported<sup>10,12</sup> local vibrational model 890  $\text{cm}^{-1}$  apart from ZPL's in emission spectra is confirmed also

by the current work (Figs. 2–4, 6, and 7). The energy of the mode, 890  $\text{cm}^{-1}$  in the ground state and 860  $\text{cm}^{-1}$  in the excited state,<sup>12</sup> is close to the calculated silicon–nonbridging-oxygen atom symmetric stretching mode energy of 850  $\text{cm}^{-1}$ .<sup>26</sup> The simplest estimate  $\omega^2 = k/m^*$ , taking the reduced mass of the Si-O molecule for the mode mass  $m^*$  and assuming the usual<sup>29</sup> Si-O stretching force constant  $K = 4.5 \times 10^5$  dyn/cm, yields 867  $\text{cm}^{-1}$ . The experimentally observed Si-O stretch vibration of a related structural unit—the bound hydroxyl group—has energy of 969  $\text{cm}^{-1}$ .<sup>30</sup> The 890- $\text{cm}^{-1}$  line is noticeably wider than the ZPL, indicating the dispersion of local vibrational mode energies for subset of centers with identical ZPL energies. The partial Huang-Rhys factor for the coupling of an electronic transition to this mode can be calculated from the ratio of the line integrals by Eq. (7). The data from the previous work<sup>12</sup> for excitation energies 1.905 and 1.92 eV give  $S = 0.06$ . The present data (Figs. 2 and 4) yield  $S = 0.04$  and 0.05, respectively. To account for the measurement noise, we put the final  $S$  value as  $S = 0.06 \pm 0.03$ . The small  $S$  value indicates that the bond length between the Si and nonbridging oxygen atom is almost the same both in ground and excited states of the center. As can be seen from Fig. 7, the relative contribution of the 890- $\text{cm}^{-1}$  mode to the phonon wing is small and coupling to the vibrations in the 100–400  $\text{cm}^{-1}$  range is much stronger. According to the calculations,<sup>26</sup> the wagging mode of the nonbridging oxygen atom has an energy around 300  $\text{cm}^{-1}$  and thus can be one of the major contributors to the phonon sideband. It is interesting to note that there is no strong coupling to the fundamental Si-O lattice mode at 1060  $\text{cm}^{-1}$ .

The other previously reported<sup>12</sup> low-energy vibrational line separated from the ZPL by 50  $\text{cm}^{-1}$  is observed in the current work as well (Figs. 2–4), but less distinctly, sometimes just as a shoulder. In the hole-burning spectra, this energy corresponds to a maximum of the PSB 50–60  $\text{cm}^{-1}$  from the ZPL (Fig. 7). The lowest-energy optical phonons in  $\alpha$ -quartz crystal observed by Raman scattering are at 128  $\text{cm}^{-1}$ ,<sup>31</sup> but the energy region of 50  $\text{cm}^{-1}$  corresponds to high-frequency acoustic phonons. In glassy  $\text{SiO}_2$ , however, a Raman peak at 50  $\text{cm}^{-1}$  is a characteristic feature.<sup>32</sup> The presence of the Raman peak in silica glass at this energy is attributed to “acoustic-phonon-like” excitations made possibly by the lack of a clear distinction between the acoustic and optical phonons in glass and by the relaxation of the wave vector selection rule in systems without translation symmetry. This peak is usually referred to as a “boson peak.”<sup>32</sup>

PSB's of the form, qualitatively similar to Fig. 7, with the maximum very close to the ZPL are commonly observed for polymers and frozen dye solutions.<sup>20</sup> We tentatively attribute the 50- $\text{cm}^{-1}$  PSB peak to interaction with acousticlike phonons in glassy  $\text{SiO}_2$ . However, the alternative possibility cannot be ruled out, that low-frequency local modes specific to this defect exist and contribute significantly to the PSB. The situation is further complicated by the possibility that the 50- $\text{cm}^{-1}$  peak in emission spectra could have partially pseudoline character—i.e., it could be due to ZPL's of centers, selectively excited in their 50- $\text{cm}^{-1}$  vibronic line in the *absorption (excitation)* spectrum. Pseudolines, however, should not contribute to the hole-burning (selective satura-

tion) spectra of Figs. 2(b), 3(b), 4(b), and 7, due to the large differences in absorption cross sections of ZPL's and vibronic lines. This could explain the relatively better pronounced (sharper)  $50\text{-cm}^{-1}$  lines in the excitation spectra<sup>12</sup> as compared to hole-burning emission spectra of Figs. 2(b), 3(b), and 4(b).

#### D. Implications to the possible alternative structural models of the $R$ center

As already mentioned in the Introduction, the structural model of the  $R$  center is still controversial (see Refs. 11 and 12 for a review). The only truly unanimously agreed point is that the  $R$  center is related to excess oxygen in silica. Apart from the NBOHC model,<sup>4,10,12</sup> it has been suggested that  $R$  center is connected to interstitial ozone molecules.<sup>6,17</sup> The presence of vibronic structures in low-temperature optical spectra of oxygen-containing crystals is often associated with some form of molecular (or molecular ion) oxygen species. Indeed, the similarities between isochronal anneal behaviors of the  $R$  band and peroxide radical EPR signals<sup>11</sup> could point to a connection between them. Inhomogeneous widths calculated from the peroxide radical EPR spectra and from the ZPL intensity distribution of the  $R$  center are comparable (Sec. IV A above). Moreover, peroxide radical is the closest relative to the interstitial  $\text{O}_2^-$  molecular ion in alkali halides, which are well known for the presence of vibronic structures in their optical spectra. Ozonide ion  $\text{O}_3^-$  type centers can exhibit vibronic structures as well. Their presence has been demonstrated by EPR in alkali silicate glasses<sup>33</sup> or fused silica powders.<sup>34</sup> Therefore, apart from the NBOHC model, the current results should be compared to the expectations derived from different alternative structural models of the  $R$  center.

##### 1. $\text{O}_2^-$ or peroxide radical

The  $890\text{-cm}^{-1}$  mode is smaller in energy than any occurrence of local vibration of  $\text{O}_2^-$  or  $X^+\text{-O}_2^-$  radical in different matrices. The O-O force constants and stretching frequencies in different  $X\text{-O}_2^-$  radicals are dependent on the degree of transfer of valence electron from the ion  $X$  to the antibonding  $\pi$  orbital of the  $\text{O}_2^-$  ion. In the series  $\text{O}_2$  (free molecule),  $\text{FO}_2$ ,  $\text{ClO}_2$ ,  $\text{HO}_2$ ,  $\text{LiO}_2$ , and  $\text{O}_2^-$  (free molecular ion), the electron transfer increases from 0% ( $\text{O}_2$ ) to 100% ( $\text{O}_2^-$ ) and the vibrational mode frequencies decrease accordingly (1560, 1490, 1440, 1090, and  $1090\text{ cm}^{-1}$ , respectively<sup>35</sup>). The matrix effects can add additional shifts of order  $100\text{ cm}^{-1}$ ; hence, the O-O stretching frequencies of any  $\text{O}_2^-$ -like species should lie in the range between 1000 and  $1600\text{ cm}^{-1}$ . For example, in different alkali halide crystals,  $\text{O}_2^-$  vibration frequencies are between 1050 and  $1110\text{ cm}^{-1}$ .<sup>36</sup>

The decisive evidence against the oxygen molecular ion  $\text{O}_2^-$  or peroxide radical model for the  $R$  center comes, however, from the difference in Huang-Rhys factors: The emission transition in  $\text{O}_2^-$  is strongly coupled to O-O vibration [ $S \approx 10$  (Refs. 25,36)], while the coupling to the  $890\text{-cm}^{-1}$  mode in the  $R$  center is very weak ( $S \approx 0.06$ ). Additionally, the decay constant of  $\text{O}_2^-$  luminescence [ $\approx 0.1\ \mu\text{s}$  at 80 K (Ref. 36)] is 100 times smaller than that of the  $R$  center (10–30  $\mu\text{s}$ ), and the energies of zero-phonon transitions in

both cases are very different:  $\approx 1.9\text{ eV}$  for the  $R$  center and  $3.2\text{--}3.3\text{ eV}$  for  $\text{O}_2^-$  in alkali halide crystals.<sup>36</sup>

##### 2. Ozonide ion $\text{O}_3^-$

The spectroscopic characteristics of another alternative to the  $R$ -center model, the ozonide ion  $\text{O}_3^-$ , have been investigated in  $\text{NaClO}_3$  crystals<sup>37</sup> by optical absorption and resonance Raman scattering. The dominant ground-state vibration energy,  $1020\text{ cm}^{-1}$ , is higher than in the  $R$  center and again the Huang-Rhys factor ( $S = 6.5$ ) is very different from that of the  $R$  center. The luminescence of  $\text{O}_3^-$  has not been observed.

##### 3. Interstitial ozone molecules

The infrared properties of ozone molecules  $\text{O}_3$ , suggested to be involved in  $R$ -band emission,<sup>6,17</sup> have been investigated in rare gas matrices.<sup>38</sup> The three fundamental vibration mode energies for  $\text{O}_3$  are at 1105, 1035, and  $705\text{ cm}^{-1}$ , different from the local mode of the  $R$  center.

On the other hand, the NBOHC model is in reasonable agreement with all of the presently known spectroscopic data on the  $R$  center. The most interesting feature of the  $R$  center revealed by the present work, the unusually small electron-phonon coupling, which cannot be satisfactorily explained by any of the alternative models, fits well in the framework of the NBOHC model, since the electron transition changes merely the population of  $2p$ -like lone pair orbitals of two neighboring oxygen atoms and thus very little relaxation occurs. The energy of the  $890\text{-cm}^{-1}$  vibronic mode is close to the value expected for the silicon–nonbridging-oxygen stretching mode. As pointed out previously,<sup>12</sup> the NBOHC model agrees as well with the radiochemical properties of the  $R$  center and with the luminescence polarization data, both under excitation in the 2.0-eV absorption band and in the controversial 4.8-eV UV absorption band.

The main controversial point with the NBOHC model is the inconsistent mutual relations between the intensities of the 1.9-eV PL and 2.0- and 4.8-eV optical absorption bands, associated with the  $R$  center, and the intensity of the NBOHC EPR signal, measured for different samples or in the isochronal anneal experiments (see Refs. 11,12 for a review). Both reasonable and poor EPR optical correlations have been obtained in different studies. Part of the reported discrepancies can be attributed to an accidental overlap of optical bands, since several different absorption bands in  $g\text{-SiO}_2$  have been reported both in the 2.0- and 4.8-eV regions. However, apart from this, a more fundamental and so far neglected reason for the observed deviations may exist. In the presence of inhomogeneous broadening, the signal intensity recorded by some arbitrary spectroscopic method is in fact the mean value, averaged over the ensemble of inequivalent centers with individual weighing factors, which are *different* for various methods used. For example, the main contribution to the PL spectra is made by the subset of centers with higher thermal quenching activation energies (higher quantum yield), while optical absorption spectra are dominated by centers with higher transition oscillator strength. In the general case, an exact proportionality between the intensities of signals, obtained in glass by different techniques, *does not exist*; the correlations are more or less approximate.

This is treated in more detail in Ref. 39. The reasonably possible extent of the deviations must be considered in each case separately. Therefore, unlike the case of monocrystals, a lack of an exact correlation between different signals in isochronal anneal experiments does not automatically prove that these signals belong to different centers.

The local site symmetry of the nonbridging oxygen atom in the zero approximation is  $C_{3v}$ , as far as only the interactions with the atoms of the same  $\text{SiO}_4$  tetrahedron are considered. This would give an electronic ground state  ${}^2E$  with both oxygen lone pair  $2p$  orbitals degenerate, in fact a Jahn-Teller system. Since both EPR work<sup>24</sup> and the present optical data show that inhomogeneous broadening effects are strong, this discrepancy is evidently lifted through random nonaxial interactions with the rest of the glass network and a distribution of the splitting energies  $\Delta E$  exists. A significant part of centers with  $\Delta E$  close to zero may exist. This can give rise to very large distributions in  $g$ -factor anisotropy and spin-lattice relaxation rates, affecting the accuracy of the EPR optical correlations through the mechanism discussed above. Indeed, the PL emission and excitation spectra of the  $R$  center are not mirror symmetric relative to the ZPL energy.<sup>12</sup> This feature often points<sup>25</sup> to a near degeneracy of the excited or ground state.

## V. CONCLUSION

The main outcome of this work is the establishing of the homogeneous shape ("single-site spectrum") of the  $R$  center. The optical absorption and PL bands of defects in silica glass are generally wide and structureless even at liquid-He temperatures and yield little structural information which could be confronted directly with different defect models. Together with the erratic EPR optical correlations these are the main

causes of the still continuing controversy over almost every optical band in silica glass.<sup>40</sup> The relatively detailed optical characterization of the  $R$  center available now gives a much better framework for selecting the defect model. The present optical data fit well with the nonbridging oxygen hole center model. However, the crucial correlation between the  $R$  band and NBOHC EPR signal and sources of the possible deviations from the linear relationship should be rechecked in the light of the improved understanding of the  $R$ -center optical properties and of the role of inhomogeneous broadening.

Apart from being a basic intrinsic defect in a technologically important material, the  $R$  center may be of a more general interest as an instance of, as far as we know, one of the weakest electron-phonon coupling strengths reported for intrinsic defects in any oxide material. Another interesting peculiarity, unlike the other basic intrinsic defect in  $g$ - $\text{SiO}_2$ , the  $E'$  center,<sup>11</sup> the  $R$  center is inherent exclusively to the glassy form of  $\text{SiO}_2$ : Despite the similarity in the near order and bonding in silica glass and  $\alpha$ -quartz, the  $R$  center has never been detected in quartz crystals, unless the crystal has been amorphized by large irradiation doses. At the same time, the  $R$  center occurs also as a surface defect,<sup>9</sup> consistent with the notion that its bulk counterpart, investigated here, is a dangling bond projecting in a microvoid in the silica glass network.

## ACKNOWLEDGMENTS

This work was supported by the Ministry of Education, Culture and Science of Japan. L.S. was additionally supported by Latvian Science Council Grant No. 93-656. L.S. is indebted to Professor Noriaki Itoh for arranging the joint work and many helpful discussions.

- 
- <sup>1</sup>A. Silin, L. Skuja, and A. V. Shendrik, *Fiz. Khim. Stekla* **4**, 405 (1978).
- <sup>2</sup>E. J. Friebele, D. L. Griscom, and M. J. Marrone, *J. Non-Cryst. Solids* **71**, 133 (1985).
- <sup>3</sup>G. H. Sigel, *J. Non-Cryst. Solids* **13**, 372 (1973/74).
- <sup>4</sup>L. Skuja, A. Silin, and A. G. Boganov, *J. Non-Cryst. Solids* **63**, 431 (1984).
- <sup>5</sup>J. H. Stathis and M. Kastner, *Philos. Mag. B* **49**, 357 (1984).
- <sup>6</sup>K. Awazu and H. Kawazoe, *J. Appl. Phys.* **68**, 3584 (1990).
- <sup>7</sup>Y. Hibino and H. Hanafusa, *J. Non-Cryst. Solids* **107**, 23 (1988).
- <sup>8</sup>P. W. Wang, R. G. Albridge, D. L. Kinser, R. A. Weeks, and N. H. Tolc, *Nucl. Instrum. Methods Phys. Res. B* **59**, 1317 (1991).
- <sup>9</sup>A. N. Streletsky, A. B. Pakovich, V. F. Gachkovsky, Yu. Aristov, Yu. Rufov, and I. Butyagin, *Khim. Fiz.* **7**, 938 (1982).
- <sup>10</sup>L. Skuja, *Solid State Commun.* **84**, 613 (1992).
- <sup>11</sup>D. L. Griscom, *J. Ceram. Soc. Jpn.* **99**, 923 (1991).
- <sup>12</sup>L. Skuja, *J. Non-Cryst. Solids* **179**, 51 (1994).
- <sup>13</sup>S. Munekuni, T. Yamanaka, Y. Shimogaichi, R. Tohmon, Y. Ohki, K. Nagasawa, and Y. Hama, *J. Appl. Phys.* **68**, 1212 (1990).
- <sup>14</sup>R. M. Atkins and P. J. Lemaire, *J. Appl. Phys.* **72**, 344 (1992).
- <sup>15</sup>L. Skuja and A. Silin, *Phys. Status Solidi A* **56**, K11 (1979).
- <sup>16</sup>R. Tohmon, Y. Shimogaichi, S. Munekuni, Y. Ohki, Y. Hama, and K. Nagasawa, *Appl. Phys. Lett.* **54**, 1650 (1989).
- <sup>17</sup>N. Kuzuu, Y. Matsumoto and M. Marahara, *Phys. Rev. B* **48**, 6952 (1993).
- <sup>18</sup>M. J. Weber, in *Laser Spectroscopy of Solids*, edited by W. M. Yen and P. M. Selzer (Springer, Berlin, 1986), pp. 189–239.
- <sup>19</sup>J. Kikas, in *Zero-Phonon Lines and Spectral Hole Burning in Spectroscopy and Photochemistry*, edited by O. Sild and A. Haller (Springer, Berlin, 1988), p. 89.
- <sup>20</sup>J. S. Ahn, Y. Kanematsu, and T. Kushida, *Phys. Rev. B* **48**, 9058 (1993).
- <sup>21</sup>J. Fuenfschilling, I. Zschokke-Graenacher, and D. F. Williams, *J. Chem. Phys.* **75**, 3669 (1981).
- <sup>22</sup>It has been alternatively proposed in Ref. 20 that the resonance ZPL excitation spectrum is proportional to  $E^4W(E)$ . The additional factor  $E^4$  [Eq. (6) in Ref. 20] comes evidently from the Einstein relation ( $\propto E^3$ ) between the spontaneous and induced transition probabilities [e.g., J. B. Birks, *Photophysics of Aromatic Molecules* (Wiley, London, 1970), p. 48]. However, the inclusion of this factor may be not necessary in our case, since the intensity of (nonsaturated) PL emission is not proportional to the PL spontaneous transition probability, but rather to the luminescence quantum yield, which by the model assumptions [Eq. (1)] is assumed to be constant for all sites.
- <sup>23</sup>F. Rasheed, K. P. O'Donnell, B. Henderson, and D. B. Hollis, *J. Phys. C* **3**, 1915 (1991).



- <sup>24</sup>M. Stapelbroek, D. L. Griscom, E. J. Friebele, and G. H. Sigel, Jr., *J. Non-Cryst. Solids* **32**, 313 (1979); D. L. Griscom (private communication).
- <sup>25</sup>B. Henderson and G. F. Imbusch, *Optical Spectroscopy of Inorganic Solids* (Clarendon, Oxford, 1989).
- <sup>26</sup>R. B. Laughlin and J. B. Joannopoulos, *Phys. Rev. B* **17**, 4922 (1978).
- <sup>27</sup>B. D. Evans and M. Stapelbroek, *Solid State Commun.* **33**, 765 (1980).
- <sup>28</sup>E. F. Martinovich, A. G. Tokarev, and S. A. Zilov, *Opt. Spektrosk.* **61**, 338 (1986) [*Opt. Spectrosc. (USSR)* **61**, 537 (1986)].
- <sup>29</sup>R. J. Bell in *Methods in Computational Physics*, edited by G. Gilat (Academic, New York, 1976), p. 215.
- <sup>30</sup>C. M. Hartwig and L. A. Rahn, *J. Chem. Phys.* **67**, 4260 (1977).
- <sup>31</sup>J. B. Bates, R. W. Hendricks, and L. B. Schaffer, *J. Chem. Phys.* **61**, 4163 (1974).
- <sup>32</sup>J. Jäckle, in *Topics in Current Physics*, edited by W. A. Phillips (Springer, Berlin, 1981), Vol. 24, p. 135.
- <sup>33</sup>R. Cases and D. L. Griscom, *Nucl. Instrum. Methods Phys. Res. B* **1**, 503 (1984).
- <sup>34</sup>V. A. Radtsig and A. B. Bistrikov, *Kinet. Katal.* **19**, 713 (1978).
- <sup>35</sup>L. Andrews, *J. Chem. Phys.* **50**, 4288 (1969).
- <sup>36</sup>A. Rebane, in *Molecular Luminescence Centers O<sub>2</sub><sup>-</sup> and S<sub>2</sub><sup>-</sup> in Alkali Halide Crystals* (Valgus, Tallin, 1968) (in Russian). Note that this reference is correct but perhaps senseless for any reader outside the former USSR. K. K. Rebane has published several English language books on this subject. If you know any English language reference on the energies of O<sub>2</sub><sup>-</sup> vibrations in different alkali halide crystals, it would be perhaps better to substitute it here.
- <sup>37</sup>J. B. Bates and J. C. Pigg, *J. Chem. Phys.* **62**, 4227 (1975).
- <sup>38</sup>L. Brewer and J. Ling-Fai Wang, *J. Chem. Phys.* **56**, 759 (1972).
- <sup>39</sup>L. Skuja, *Glastech. Ber.* **67C**, 334 (1994).
- <sup>40</sup>The only exception is the widely accepted correlation of the E'-center EPR signal to the 5.8-eV absorption band [R. A. Weeks and E. Sonder, in *Paramagnetic Resonance*, edited by W. Low (Academic, New York, 1963, Vol. 2, p. 869)]. However, absorption bands of different origin at 5.8 eV as well [e.g., R. A. Weeks, R. H. Magruder III, and P. W. Wang, *J. Non-Cryst. Solids* **149**, 122 (1992)].